

## Oxide Shell Assisted Vapor–Liquid–Solid Growth of Periodic Composite Nanowires—A Case of Si/Sn

Hui Wang,<sup>†,‡</sup> Xiao Hong Zhang,<sup>\*,‡</sup> Chu Sing Lee,<sup>†</sup> Kai Zou,<sup>‡</sup> Wen Sheng Shi,<sup>‡</sup>  
Shi Kang Wu,<sup>‡</sup> Jack Chang,<sup>†,‡</sup> and Shuit Tong Lee<sup>\*,†,‡</sup>

Center of Super-Diamond and Advanced Films and Department of Physics and Materials Science, City University of Hong Kong, Hong Kong SAR, China, and Nano-organic Photoelectronic Laboratory and Laboratory of Organic Optoelectronic Functional Materials and Molecular Engineering, Technical Institute of Physics and Chemistry, Chinese Academy of Sciences, Beijing 100101, China

Received June 20, 2007. Revised Manuscript Received August 6, 2007

In the conventional vapor–liquid–solid (VLS) growth process, the wires or whiskers grown from the liquid catalyst droplets are always in the solid state. Here, we report the synthesis of a silicon-based periodic nanowire structure using a periodic volume-changing Sn particle as catalyst. Contrary to the common VLS process, the nanostructure growth was instead governed by a catalyst head consisting of a mixture of solid and liquid, and liquid Sn segments periodically appeared in Si nanowires during the growth process. The liquid Sn segments catalyzed the growth of secondary or branching nanowires from the primary nanowires. The result reveals clearly that the unusual growth is governed by the dual action of VLS and oxide-assisted growth (OAG). It further suggests a new pathway to rational design and synthesis of periodic composite nanostructures by taking advantage of both VLS and OAG processes.

The vapor–liquid–solid (VLS) growth is widely used to prepare one-dimensional nanostructures.<sup>1–10</sup> In this approach, the material constituting the nanowire vaporizes at a high temperature and then condenses at a low temperature to form liquid alloy droplets with a nanoscale metal catalyst particle (such as Au, Fe, etc.). The liquid droplets serve as the preferred sites for condensation and dissolution of the incoming vapor.<sup>11–12</sup> Once the absorbed material becomes supersaturated in the liquid alloy droplets at a given temperature, it segregates from the droplet to form nuclei. Further segregation and subsequent axial growth of the nuclei would lead to the formation of 1-D nanostructures. According to the typical VLS mechanism, only the solid phase can grow up from the molten alloy droplet, and once 1-D structures are formed, their general morphologies are mostly deter-

mined. Continual growth of the 1-D structures invariably leads to an increase in length and sometimes slight changes in diameter.<sup>13</sup> Oxide-assisted growth (OAG) is another popular growth process for the synthesis of semiconductor nanostructures, which has been especially successful for Si nanowires.<sup>14–18</sup> In this process, no metal catalyst is needed to form the low-temperature alloy droplet. In OAG, the nanosized oxide tip at the end of the nanostructure plays the role of metal catalyst because of its low melting point due to the small size effect.<sup>15</sup> Another notable characteristic of OAG is the amorphous oxide shell, which sheaths the crystalline core and limits the lateral dimension of the nanostructure. In the present work, we synthesized a unique Si–Sn regular 1-D nanostructure through periodically adjusting the concentration of the incoming material in the leading droplet by repeatedly changing its volume, and we also explored its growth mechanism. We found that the presence of a solid spherical ball and liquid segments in the final 1-D nanostructure cannot be explained by either the VLS or the OAG process alone. Instead, the growth can be considered to be a VLS process driven by an oxidation–reduction reaction, in which the oxide shell together with the surface tension of the leading alloy droplet causes the liquid phase to move downward. This finding extends the application of

\* Corresponding authors. (X.Z.) Fax: +86 10 648 79375; E-mail: xhzhang@mail.ipc.ac.cn. (S.-T.L.) Fax: +852 278 44696; e-mail: apannale@cityu.edu.hk.

<sup>†</sup> City University of Hong Kong.

<sup>‡</sup> Chinese Academy of Sciences.

- (1) Wagner, R. S.; Ellis, W. C. *Appl. Phys. Lett.* **1964**, *4*, 89–90.
- (2) Huang, M. H.; Wu, Y.; Feick, H.; Tran, N.; Weber, E.; Yang, P. *Adv. Mater.* **2001**, *13*, 113–116.
- (3) Jiang, Y.; Meng, X. M.; Liu, J.; Hong, Z. R.; Lee, C. S.; Lee, S. T. *Adv. Mater.* **2003**, *15*, 1195–1198.
- (4) Bonard, J. M.; Chauvin, P.; Klinke, C. *Nano Lett.* **2002**, *2*, 665–667.
- (5) Gu, G.; Burghard, M.; Kim, G. T.; Dsüberg, G. S.; Chiu, P. W.; Krstic, V.; Roth, S.; Han, W. Q. *Appl. Phys. Lett.* **2001**, *90*, 5747–5751.
- (6) Wu, Y.; Messer, B.; Yang, P. *Adv. Mater.* **2001**, *13*, 1487–1489.
- (7) Duan, X.; Lieber, C. M. *Adv. Mater.* **2000**, *12*, 298–302.
- (8) Liang, C. H.; Meng, G. W.; Lei, Y.; Philipp, F.; Zhang, L. D. *Adv. Mater.* **2001**, *13*, 1330–1333.
- (9) Gudiksen, M. S.; Lathon, L. J.; Wang, J.; Smith, D. C.; Lieber, C. M. *Nature (London, U.K.)* **2002**, *415*, 617–620.
- (10) Björk, M. T.; Ohlsson, B. J.; Sass, T.; Persson, A. T.; Thelander, C.; Magnusson, M. H.; Deppert, K.; Wallenberg, L. R.; Samuelson, L. *Nano Lett.* **2002**, *2*, 87–89.
- (11) Wu, Y.; Yang, P. *J. Am. Chem. Soc.* **2001**, *123*, 3165–3166.
- (12) Zhan, J.; Bando, Y.; Hu, J.; Sekiguchi, T.; Golberg, D. *Adv. Mater.* **2005**, *17*, 225–230.

- (13) Gudiksen, M. S.; Wang, J. F.; Lieber, C. M. *J. Phys. Chem. B* **2001**, *105*, 4062–4064.
- (14) Wang, N.; Tang, Y. H.; Zhang, Y. F.; Lee, C. S.; Lee, S. T. *Phys. Rev. B* **1998**, *58*, 16024–16026.
- (15) Lee, S. T.; Zhang, Y. F.; Wang, N.; Tang, Y. H.; Bello, I.; Lee, C. S. *J. Mater. Res.* **1999**, *14*, 4503–4507.
- (16) Zhang, R. Q.; Lifshitz, Y.; Lee, S. T. *Adv. Mater.* **2003**, *15*, 635–640.
- (17) Shi, W. S.; Zheng, Y. F.; Wang, N.; Lee, C. S.; Lee, S. T. *Adv. Mater.* **2001**, *13*, 591–594.
- (18) Zhang, Y. F.; Tang, Y. H.; Wang, N.; Yu, D. P.; Lee, C. S.; Bello, I.; Lee, S. T. *Appl. Phys. Lett.* **1998**, *72*, 1835–1837.

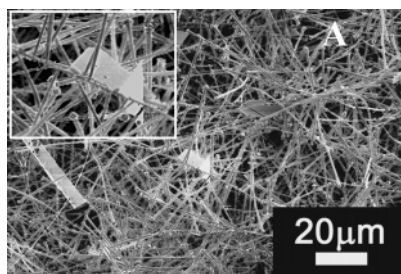


**Figure 1.** SEM image of as-deposited nanostructure. An enlarged section of the picture is shown in the upper left corner.

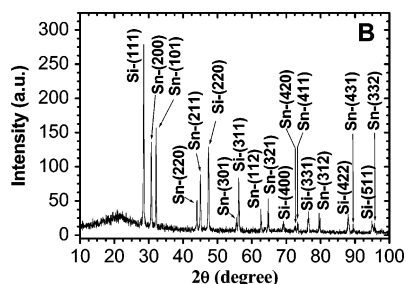


**Figure 2.** XRD pattern of as-deposited nanostructure.

the VLS mechanism, provides a rational basis for the growth of other periodic 1-D nanostructures, and offers a potential pathway to design novel composite nanomaterials with metal–semiconductor interfaces.

The morphology of the as-deposited nanostructure is shown in Figure 1. The wire-like structures have an average diameter of about 500 nm and a length of hundreds of micrometers. Nanostructures with branches on the primary trunks also can be found (inset in Figure 1). X-ray diffraction (XRD) patterns of the as-synthesized composite nanowires show that the sample is dominated by a cubic silicon and body-centered Sn phase (Figure 2). The weak broad peak centered at  $21^\circ$  in this pattern is attributed to amorphous  $\text{SiO}_x$ .

The sample was further characterized with transmission electron microscopy (TEM). TEM images in Figure 3A,B show that each wire is periodically segmented with dark dots separated roughly  $2 \mu\text{m}$  from each other. Branching of the primary wires can be observed at some dark spots. Figure 3B reveals a wire with a polyhedron ball at its tip, while one of the dark dots is magnified and is shown in Figure 3C as site a. From the magnified image, it can be clearly seen that the wire has a core–shell structure (the diameter of the core is about 250 nm). The selected-area electron diffraction (SAED) pattern (inset of Figure 3C) obtained from site b in Figure 3C shows that the core is crystalline and that the shell is amorphous. An energy dispersive X-ray (EDX) spectrometer attached to the TEM instrument was used to analyze the chemical compositions at sites b and a, and the results are shown in Figure 3D,E, respectively. The EDX spectrum in Figure 3E indicates that the dark dot a has a high content of Sn and a little O and Si (atom ratio of Sn/O/Si is about 4:3:2), where the O and Si signals may have come from the  $\text{SiO}_x$  shell. The EDX spectrum of site b (Figure 3D) shows only peaks from Si and O (atom ratio of Si/O is 1.5:~1). The oxygen signal may have come from the outer shell of  $\text{SiO}_x$ , while the core is crystalline Si. Thus, the periodic dark dots in the nanowires are Sn segments, which are expected

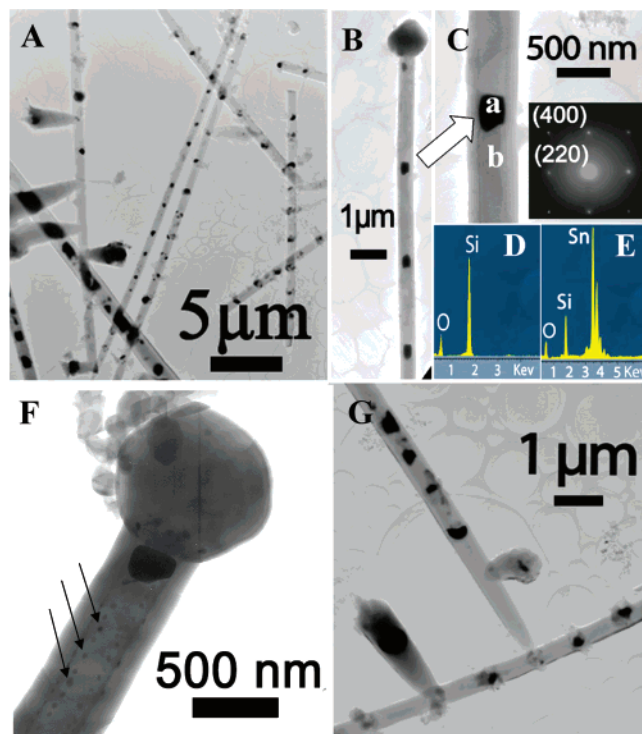


**Figure 3.** (A) TEM image of as-deposited nanostructure with a periodical structure. (B) TEM image of a whisker with a spherical ball on the tip. (C) Magnified TEM image of the section with a dark dot; the inset shows the SAED pattern at site b. (D and E) EDX spectra recorded at sites a and b. (F) TEM image of a typical polyhedron tip. (G) TEM image of the Si/Sn periodical nanostructure showing nanowire branching from a dark spot.

to be in a liquid state during the growth process (at about  $1000^\circ\text{C}$ ) because of the low melting point of Sn ( $231^\circ\text{C}$ ).

The polyhedron balls at the end of the nanowires were studied with TEM and EDX since the metallic tip of the wire is considered to be a signature of the VLS process. EDX spectra obtained from the balls show different atomic proportions of Si and Sn at different locations. The different contrast inside the polyhedron ball (Figure 3B,F) suggests inhomogeneous composition, which may be due to phase separation of the metal alloy droplet at the end of the experiment during the temperature ramp down. In addition, analysis showed that almost all the polyhedrons at the tip are actually silicon particles with some Sn-rich dots trapped inside (Figure 3F). EDX results of the particles show that the total content (by weight) of the high melting point Si is at least 4 times larger than that of the low melting point Sn. According to the phase diagram of Si and Sn,<sup>19</sup> the saturation concentration of liquid Si in Sn at the growth temperature ( $1000\text{--}1100^\circ\text{C}$ ) is no more than 2% and even lower at lower temperatures. Therefore, the high Si concentration content in the polyhedron indicates that the tip could only be a solid during the growth process. The question then arises as to how such a solid particle can incorporate materials and make the nanostructure grow. We note that growth is a dynamic process, in which vapors of  $\text{SiO}$  and Sn continue to evaporate from the source and condense onto the Sn–Si tips.<sup>23–25</sup>

(19) Massalski, T. B.; Okolomoto, H.; Subramanian, P. R.; Kacprzak, L. *Binary Alloy Phase Diagrams*, 2nd ed.; William W. Scott, Jr.; ASM International: Materials Park, OH, c1990 (2001 printing); p 3362.

(20) Morales, A. M.; Lieber, C. M. *Science* **1998**, *279*, 9, 208–211.

(21) Yao, Y.; Li, F. H.; Lee, S. T. *Chem. Phys. Lett.* **2005**, *406*, 381–385.

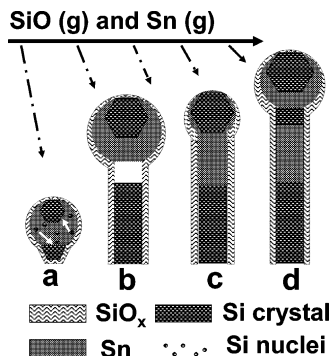


**Figure 4.** Proposed growth process of Sn/Si periodical hierarchical structures.

During growth, the liquid Sn and solid Si particles intermix and coalesce into a larger volume. As solid Si is 3 times lighter than liquid Sn (the densities of liquid Sn and solid Si are 6.983 and 2.330 kg m<sup>-3</sup>, respectively), Si nuclei would float at the upper core of the tip, where tiny nuclei would disappear and form larger particles. One such Si particle would break out from the droplet and start the nanowire growth, while others would form a larger particle floating on the tip (Figure 4a). The Si dissolved in Sn will continue to form the Si nanowire following the VLS process. Figure 3F clearly shows the Sn segment that bridges the polyhedron tip and the wire-like trunk, as well as small Sn dots close to the SiO<sub>x</sub> shell. While it is unclear as to what determines the particle or wire morphology, we suspect that the SiO<sub>x</sub> shell would play an important role<sup>26</sup> since the wire-like trunk is almost completely coated by a thick SiO<sub>x</sub> shell and practically no oxygen is found in the polyhedron tip.

Although the modified VLS mechanism could account for the formation of the Si-rich head and the silicon-based nanowires, it nevertheless cannot explain the formation of the periodic Sn dots and nanowire branches stemming from the Sn dots (Figure 3A,G), and further elucidation is needed. We suggest that the periodic Sn dots are formed due to two concerted driving forces: (1) surface tension of the liquid catalyst droplet and (2) the siphoning or capillary effect arising from the SiO<sub>x</sub> tube (details to be described later).<sup>27–28</sup> Once formed, the Sn segment can act as the catalyst for the growth of branches from nanowires. On the basis of the VLS mechanism and TEM and EDX results, we propose a growth model of the Si–Sn periodic hierarchical structure as follows, with the main processes shown schematically in Figure 4.

(1) Disproportionation and alloying: the vapors of SiO and Sn from the high-temperature region (1320 °C) condense at the low-temperature area (1000–1100 °C) and form a

liquid eutectic alloy droplet, and then SiO disproportionates into Si and SiO<sub>2</sub>. Si and SiO<sub>2</sub> subsequently phase separate, and SiO<sub>2</sub> floats on the surface of the liquid alloy droplet.<sup>29</sup> In the beginning of the process, SiO<sub>x</sub> would form faster, while Si would dissolve in the liquid Sn. Thus, the tail of the wire is essentially SiO<sub>x</sub> as described in the similar system of Ge/SiO<sub>x</sub>.<sup>32</sup>

(2) Anisotropic growth and Si phase migration: as the Si concentration in the liquid alloy droplet increased, two or more Si nuclei would separate out from the alloy ball. One of them would grow into a 1-D nanostructure via the VLS mechanism, while the others would float to the top of the liquid alloy droplet and become a regular polyhedron particle (Figure 4a).

(3) VLS growth: as Sn continually adsorbed into the tip together with SiO, and nanowire formation continually decreased the Si concentration, eventually the VLS growth would stop.<sup>31</sup> The surface tension between SiO<sub>x</sub> and liquid Sn would continually stack SiO<sub>x</sub> at the original direction, while the Si dissolved in the alloy droplet would deposit on the suspended particles or form the Si nanowire at the same time. As a result, the Si nanowire would grow slower than the SiO<sub>x</sub> tube shell. Therefore, the liquid droplet would be lifted up by the oxide tube and separated from the trunk, leading to the formation of a cavity between them (Figure 4b).<sup>30</sup>

(4) Formation of heterojunction segment: the adsorption of Sn and SiO would induce the continual growth of the droplet, which would have the inclination to become smaller to relax the increased surface energy due to the volume increase. Thus, there is a driving force to squeeze the liquid Sn downward (Figure 4c). Simultaneously, due to the lower pressure in the cavity, the Sn droplet would also experience a sucking force into the cavity. Similar capillarity-induced filling of nanotubes by liquid Sn and other materials has been reported,<sup>27,28</sup> and 1-D nanowires growing from the single catalyst droplet have been observed in both Si and Sn–ZnO system.<sup>23–25</sup> Such cavity formation would be favored by the wetting of the Sn with SiO<sub>x</sub>. These effects would occur periodically and lead to the formation of periodic Sn segments in the nanostructure.

(5) Reactivation of VLS growth: after Sn flowed into the nanowire body, the residual liquid in the tip became smaller and easier to be supersaturated. With more SiO vapor absorbed into it, another segment of the Si crystal whisker would begin to grow at the interface of the oxide tube and the droplet. Additional growth of the Si nucleus would seal the liquid column that had been sucked into the cavity and start another growing cycle (Figure 4d). Consequently, this process would produce the periodic nanostructure, while the

- (22) Pan, Z. W.; Dai, S.; Beach, D. B. *Appl. Phys. Lett.* **2003**, *83*, 3159–3161.  
 (23) Zhu, Y. Q.; Hsu, W. K.; Grobert, N.; Terrones, M.; Terrones, H.; Kroto, H. W.; Walton, D. R. M.; Wei, B. Q. *Chem. Phys. Lett.* **2000**, *322*, 312–320.  
 (24) Wang, H.; Zhang, X. H.; Meng, X. M.; Zhou, S. M.; Wu, S. K.; Shi, W. S.; Lee, S. T. *Angew. Chem., Int. Ed.* **2005**, *44*, 6934–6937.  
 (25) Ding, W.; Gao, P. X.; Wang, Z. L. *J. Am. Chem. Soc.* **2004**, *126*, 2066–2072.  
 (26) Kodambaka, S.; Hannon, J. B.; Tromp, R. M.; Ross, F. M. *Nano Lett.* **2006**, *6*, 1292–1296.  
 (27) Ajayan, P. M.; Iijima, S. *Nature (London, U.K.)* **1993**, *361*, 333–334.  
 (28) Ugarte, D.; Chtelain, A.; De Heer, W. A. *Science* **1996**, *274*, 1897–1899.

- (29) Zhang, R. Q.; Zhao, M. W.; Lee, S. T. *Phys. Rev. Lett.* **2004**, *93*, 95503-1–95503-4.  
 (30) Pan, Z. W.; Dai, Z. R.; Ma, C.; Wang, Z. L. *J. Am. Chem. Soc.* **2001**, *124*, 1817–1822.  
 (31) Our further study reveals that when bulk Sn is used as catalyst, the elemental Si produced from SiO disproportionation would completely dissolve in the bulk liquid Sn without precipitation; therefore, VLS growth would be stopped. Otherwise, SiO<sub>2</sub> nanoparticles would float on the liquid Sn surface and act as active nuclei for further growth of silica nanowires and form a highly ordered silica nanowire array on the liquid Sn surface.



frequency of the period would be determined by the rate of transport of vapors, rate of disproportionation of SiO, and solubility of Si in liquid Sn.

(6) Formation of branches: if SiO could penetrate the oxide shell and attach to the liquid Sn segments, the branching growth of nanowires would be initiated. The repeated action of such growth would produce a highly branched composite hierarchical nanostructure of periodic Sn/Si nanowires (Figure 3F).

Another possible mechanism for the formation of Sn segments is to consider that Sn dissolved in the solid silicon wires at the formation temperature (about 1000 °C) would precipitate out upon cooling. However, this mechanism fails to account for the large weight fraction of Sn in the wire. According to the phase diagram of Si and Sn, at the growth temperature, less than 0.1% (by weight) of Sn can dissolve in the silicon wire. But, the >30% weight fraction of Sn (estimated from the volume fraction and density of Sn and Si) in the wires is obviously beyond what the low Sn solubility can rationalize. On the other hand, we speculate that the tiny dark dots marked by arrows in Figure 3F may be attributed to Sn precipitation.

We suggest that the present surface tension-mediated volume-changing growth model of periodic nanostructures can similarly explain the formation of other reported structures, such as Ge–Si–SiO<sub>x</sub>, Ga–ZnS–SiO<sub>x</sub>, and In–Si–SiO<sub>x</sub>.<sup>32–34</sup> The common features among them are the disproportionation reaction of SiO and the low melting point component in the source. Actually, these reaction-driven VLS growths are dictated by both chemical and physical processes. The chemical process of disproportionation of SiO supplies Si and SiO<sub>x</sub> for the growth, while the growth rate is controlled by the rate of disproportionation of SiO and the solubility of Si in the low melting metal. At the same time, the physical

process of wetting and volume contraction by surface tension dictate the morphology of the nanomaterials. By judicious choice of the chemical and physical processes, and controlling the chemical components and growth conditions, we can expect to design new nanostructures with proper heterojunctions that may lead to new devices and applications.

### Experimental Procedures

The Sn/Si periodical hierarchical structures were synthesized using a high-temperature tube furnace with a gas flow controlling system. An alumina boat loaded with a mixture of 2.0 g of SiO (Aldrich, 325 mesh, 99.9%) and 0.5 g of Sn was placed at the center of an alumina tube (with an outside diameter of 42 mm and a length of 800 mm). The tube was then mounted inside the furnace. The temperature inside the alumina tube was measured by a movable thermocouple. The tube was first pumped to 510<sup>-2</sup> mbar and then heated at a rate of 40 °C/min to 1320 °C and maintained at this temperature for 7 h. A mixture of argon (95%) and hydrogen (5%) continually flowed through the tube at 10 sccm and a pressure of 350 mbar. After 7 h of growth at 1320 °C, the system was cooled to room temperature naturally. A gray product was obtained on the inner wall of the alumina tube as well as on a silicon wafer placed 20 cm downstream from the source materials. The temperature at the deposition zone was measured to be 1000–1100 °C with a thermocouple. We point out that the growth temperature can dramatically affect the morphology of the products, so that a different nanostructure was obtained at 750–850 °C, as we described elsewhere.<sup>24</sup> The as-deposited product was studied with scanning electron microscopy (SEM; Philips XL 30 FEG). The deposition product was dispersed in ethanol, and a drop of the dispersion was put on a carbon-coated copper TEM sample grid for examination by TEM (Philips, CM20, operated at 200 kV).

**Acknowledgment.** This work was supported by a Central Allocation Grant from the Research Grants Council of Hong Kong SAR (CityU 3/04C), the CAS-Croucher Funding Scheme for Joint Laboratories of the Croucher Foundation, the National Basic Research Program of China (973 Program) (Grant 2006CB933000), and the National High-tech R&D Program of China (863 Program) (Grant 2006AA03Z302).

CM071651Y

(32) Meng, X. M.; Hu, J. Q.; Jiang, Y.; Lee, C. S.; Lee, S. T. *Appl. Phys. Lett.* **2003**, *83*, 2241–2243.

(33) Hu, J. Q.; Bando, Y.; Zhan, J. H.; Golberg, D. *Adv. Mater.* **2005**, *17*, 1964–1969.

(34) Zhan, J. H.; Bando, Y.; Hu, J. Q.; Liu, Z. W.; Yin, L. W.; Golberg, D. *Angew. Chem., Int. Ed.* **2005**, *44*, 2140–2144.